INTERNATIONAL JOURNAL OF INTEGRATED ENGINEERING
ISSN: 2229-838X e-ISSN: 2600-7916

IJIE

Vol. 17 No. 7 (2025) 134-143
https://publisher.uthm.edu.my/ojs/index.php/ijie

The Effect of Shear Connectors on Cold-Formed Steel as Hybrid Beam Reinforcement

Indriyani Puluhulawa[1]*, Alamsyah[1], Ajeng Listianti[2]

[1] *Department of Civil Engineering, Politeknik Negeri Bengkalis, Riau 28714, INDONESIA*
[2] *Department of Civil Engineering, Universitas Tadulako, Central Sulawesi 94148, INDONESIA*

*Corresponding Author: indriyani_p@polbeng.ac.id
DOI: https://doi.org/10.30880/ijie.2025.17.07.014

Article Info

Received: 15 Mac 2025
Accepted: 3 November 2025
Available online: 31 December 2025

Keywords

Shear connector, hybrid beam, cold-formed steel

Abstract

Hybrid beams are critical components in structural engineering, often reinforced with high-tensile-strength materials that surpass conventional reinforcement bars. Cold-Formed Steel (CFS) is a commonly utilized material in this context, offering enhanced structural performance, durability, and load-bearing capacity. However, previous studies indicate that the incorporation of the CFS in hybrid beams often leads to a strength reduction of approximately 50% compared to theoretical expectations. This discrepancy is primarily attributed to slippage between the CFS and concrete, resulting from the smooth surface texture of the CFS, which limits effective bond formation. To address these challenges, shear connectors are proposed to enhance the CFS-concrete bond, aiming to boost load-carrying capacity. Therefore, this study aims to investigate hybrid beams reinforced with the CFS, focusing on ultimate load, deflection, ductility, and failure patterns. Six beams, varying in the CFS shape and shear connector type, underwent 3-point flexural testing. The results showed an impressive increase in ultimate load, of approximately 87.33%, and notable deflection reductions, ranging from 15.4% to 81.9%, compared to control beams. However, beam ductility decreased significantly, with the largest reduction observed at 78.83%, while flexural failure remained the predominant mode across all specimens.

1. Introduction

A hybrid reinforced concrete (RC) beam is a structural beam that incorporates additional materials or elements, often with higher tensile strength, to enhance its performance characteristics. The strengthening of hybrid beams is currently often carried out by using materials with higher tensile strength than conventional reinforcement steel. In line with the development of material technology, other materials have greater yield strength and tensile strength than ordinary reinforcing bars, namely Cold-Formed Steel (CFS). These bars have high tensile strength and light properties compared to ordinary steel because it has a skinny cross-section. With advancements in construction technology, the CFS is increasingly utilized in secondary structural elements that complement the main structure, enhancing overall efficiency and durability [1]. Many utilise CFS not only for truss frames in roofs but also in other structural elements. Alenezi et al. [2] investigated its use in columns reinforced with ferrocement. Taheri et al. [3] explored the CFS application in beams designed to withstand bending loads. Additionally, Puluhulawa et al. [4] examined its effectiveness in reinforcing existing floor slabs. Moreover, Kadir et al. [5] studied its use as braces for house walls. These studies demonstrate the diverse applications of CFS in

construction, showcasing its versatility and potential for enhancing structural strength and stability in various building elements.

The CFS components and structures are increasingly being used in the construction industry due to their outstanding structural and economic characteristics. The use of the CFS has reduced steel consumption by approximately 50%, construction time by up to 60%, and construction costs by up to 25%. The advantages of using the CFS include its lightweight nature, ease of connection, dimensional stability, simple implementation and transportation, and cost-effectiveness [6]. Other advantages of the CFS are : (i) high strength and rigidity, (ii) quick and easy to transport and install, (iii) reduced weather delays, (iv) no formwork required, (v) easy to cut, (vi) uniform size, (vii) capable of accommodating tolerances, and (viii) which also have a variety of shapes and configurations. The CFS sectional thicknesses typically range from 1.2 mm to 3.2 mm, with cold-formed members with a typical yield stress of 350 MPa to 550 MPa [7].

The problem with the CFS is the presence of local buckling on the web or flange that occurs due to bending loads. Therefore, several studies have focused on adding restraints to the CFS in resisting bending including adding lightweight concrete as a stiffener to the CFS with a C-shape, the result is an increase in flexural stiffness, flexural capacity, and ductility performance [8].

The use of CFS as additional tensile and shear reinforcement in beams has been attempted previously, but the results have only reached approximately 50-60% of the theoretical expectations [9]. This might be attributed to slippage occurring in the CFS as a flexural reinforcement, given that it has a relatively smooth surface [10].

From the problem descriptions, modifying the surface of the CFS appears to be the primary solution to address these issues. The addition of shear connectors to mitigate slippage on the light steel surface can be achieved by adding bolts and utilizing the light steel itself to create a rough surface. This approach has been previously demonstrated by Irwan et al. [11], in the context of composite the CFS beams and RC floor slabs. The bond between the light steel beam and the RC floor slab can be enhanced through the use of bolts and modifications to the light steel section itself, improving structural integrity and load transfer efficiency. The objective of this study is to investigate the behavior of hybrid beams strengthened with the CFS, determine the extent of the increase in flexural capacity of the CFS of -reinforced hybrid beams, and evaluate the deflection, ductility, and failure modes of these beams.

2. Materials and Methods

2.1 Initial Analysis and Beam Dimension Determination

The initial phase of this study involves analyzing to determine the dimensions of the beam and the quantity of reinforcements required, considering the maximum load capacity of the laboratory equipment. In terms of the steel and concrete quality, this preliminary analysis relies on theoretical values derived from previous research findings. The result of this initial analysis establishes the dimensions of the beam as 150 x 250 x 1300 mm. This beam is reinforced with 2ϕ8mm bars for tension, 2ϕ5 mm bars for compression, and ϕ5 - 200 mm stirrups. Additionally, two shapes of cold-formed steel are utilized, such as rectangular with dimensions of 50x0.75 mm and U-shaped obtained from the CFS C75x0.75mm, commonly used in roof truss structures. The placement of the CFS is meticulously arranged to fit the small beam dimensions and avoid interference with the concrete compacting process. This phase overlooks the potential issue of slippage between the CFS and concrete. To anticipate this problem, shear connectors from the CFS web, formed as squares and triangles, as well as self-drilling screws, are utilized.

Fig. 1 shows information on the stress-strain distribution in the CFS hybrid beams for analyzing the load or moment of the CFS hybrid beams. T_{cfs1} and T_{cfs2} represent the resultant tensile forces in the CFS, T_{s1} represents the resultant tensile force in steel reinforcement, and Cc represents the resultant compressive force in concrete. Details of the reinforcements and the beam's cross-section are shown in Fig. 2.

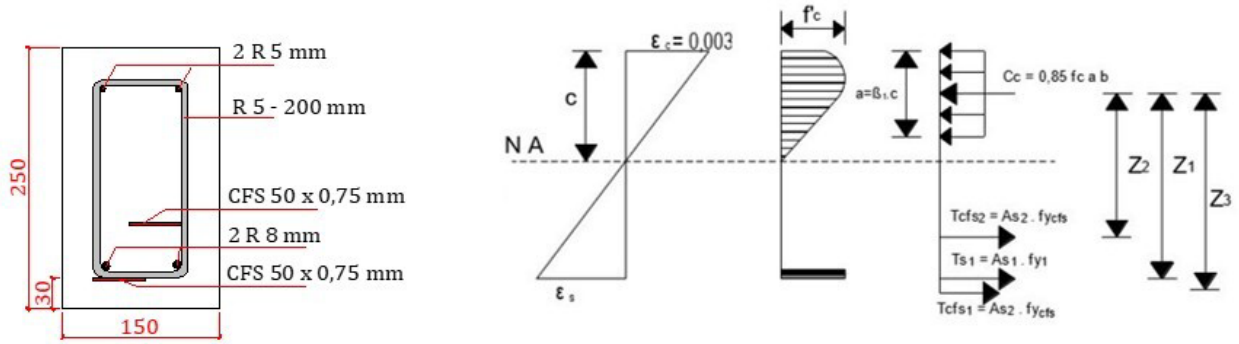

Fig. 1 *Stress-strain distribution in the CFS hybrid beam*

Int. Journal of Integrated Engineering Vol. 17 No. 7 (2025) p. 134-143

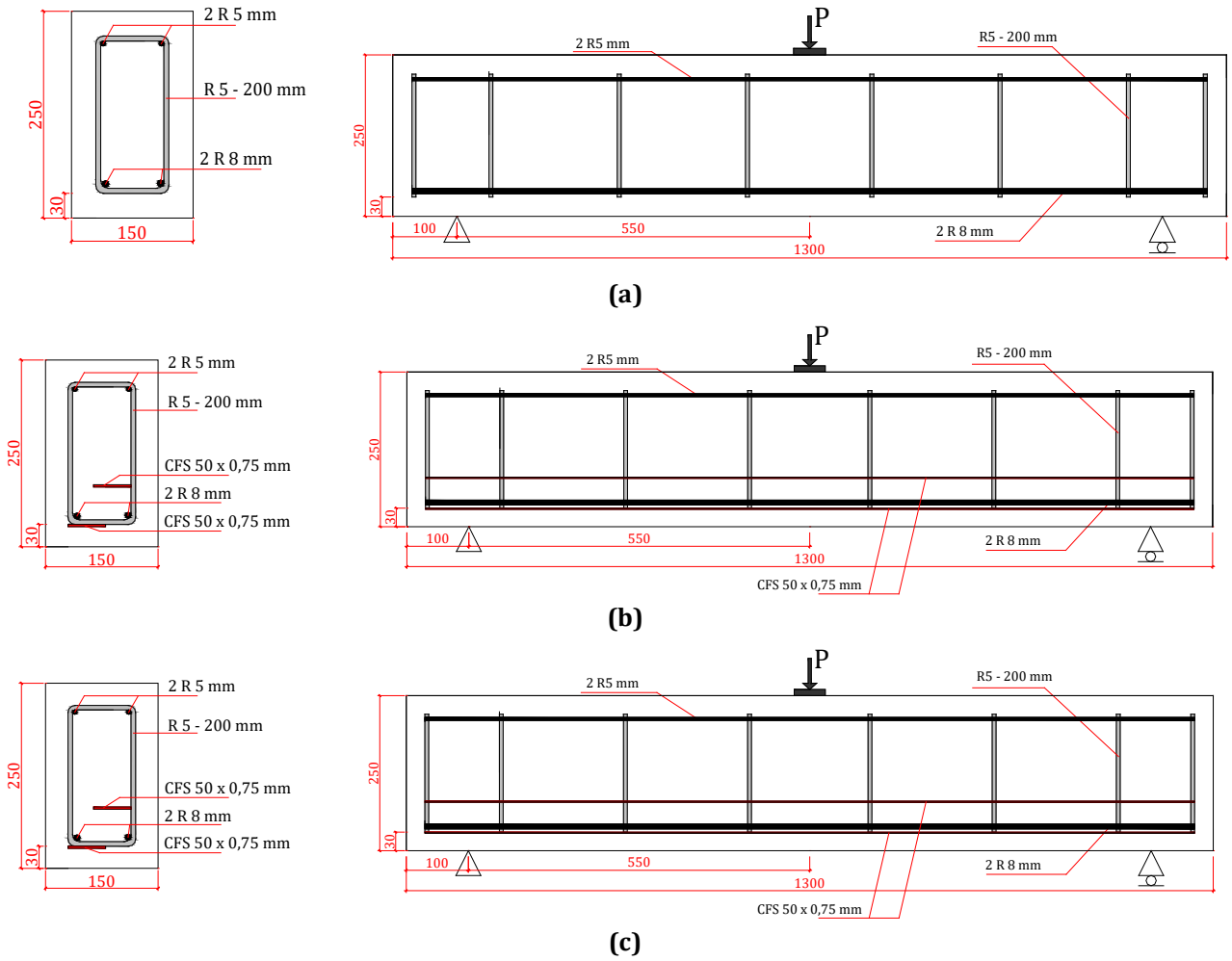

Fig. 2 *Details of specimens - (a) Controlled beam; (b) Hybrid beam with plate-shaped the CFS; and (c) Hybrid beam with U-shaped CFS*

2.2 Mix Design Composition

The next step in determining the composition of a concrete mix with a strength of 25 MPa is to refer to the Indonesian National Standard [12]. The composition of the concrete mix per cubic meter used consists of 386.7 kg of cement, 205 kg of water, 606 kg of sand, and 1177 kg of coarse aggregates.

2.3 Preparation of Specimens

In the CFS, shear connectors in the form of self-drilling screws with a diameter of 4 mm (see Fig. 3), are installed, with square and triangular shapes measuring 10x10mm. The square and triangular shear connectors are fabricated on the CFS itself. The quantity and spacing of the shear connectors are calculated based on Cui et al. [13], by initially conducting shear testing of the drilling screws with the CFS according to Lin et al. [14]. Details of the shear connectors used can be seen in Fig. 4.

Fig. 3 *Self-drilling screw as stud connector*

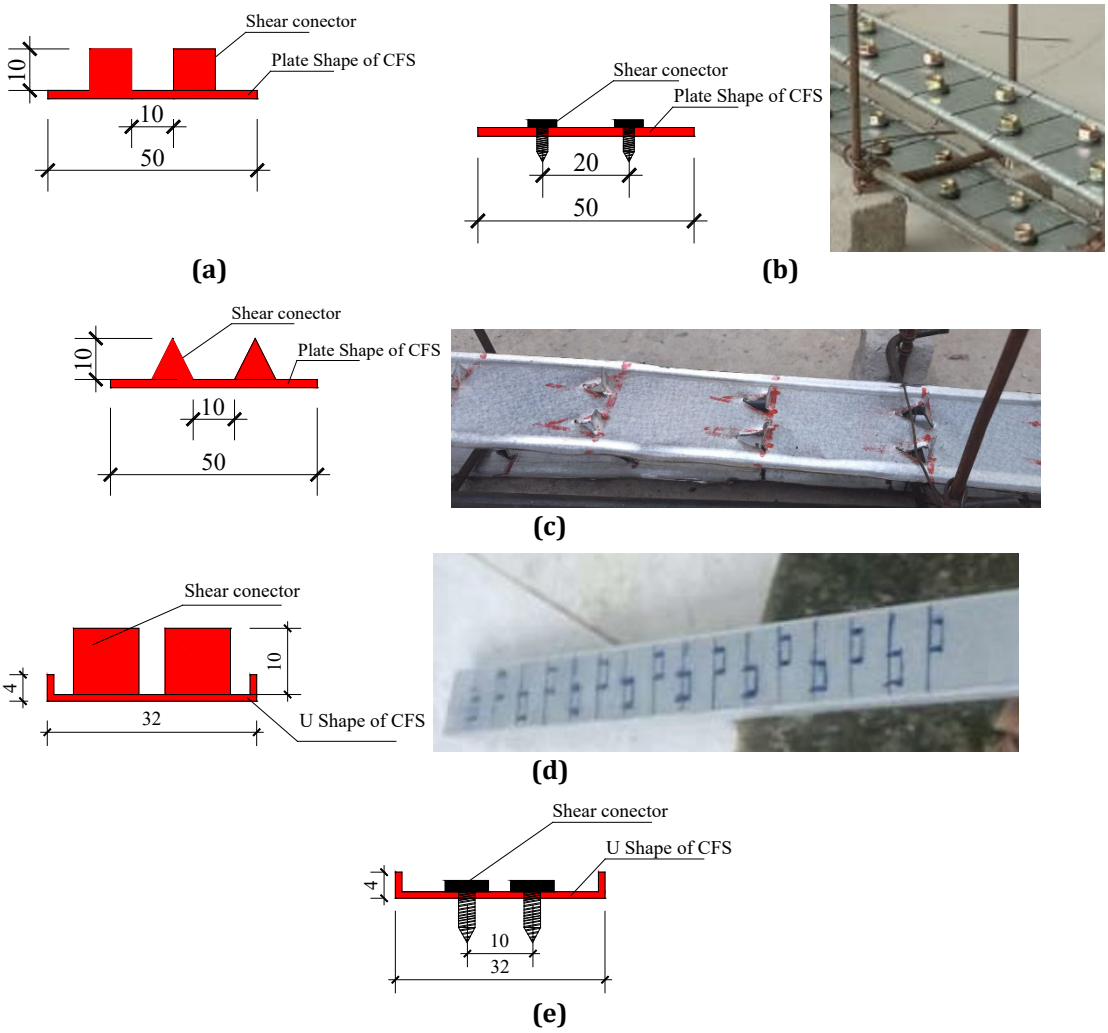

Fig. 4 *Details of the shear connectors - (a) HPS2;(b) HPS1; (c) HPS3; (d) HUS2; and (e) HUS1*

One control beam and five hybrid beams were fabricated as samples. The variations in the hybrid beams were based on the CFS shape and shear connector variations. Details and the number of test specimens that have been prepared can be seen in Table 1. Subsequently, concrete mixtures were mixed with a slump value ranging from 75-120 mm. During the pouring process, concrete cylinders were also cast to determine the actual concrete quality. The care for the concrete beam specimens was carried out by covering specimens with burlap sacks and watering for 28 days to prevent cracking due to the heat of hydration from the cement.

Table 1 *Specimens specification*

Name of Specimens	Number of specimens	Beam size (mm)	Shear connector
Control Beam (CB)	1	150 × 250 × 1300	-
Hybrid beam with plate shape of CFS (HPS1)	1	150 × 250 × 1300	Self-drilling screw diameter 4 mm
Hybrid beam with plate shape of CFS (HPS2)	1	150 × 250 × 1300	Square, size 10 × 10 mm
Hybrid beam with plate shape of CFS (HPS3)	1	150 × 250 × 1300	Triangle, size 10 × 10mm
Hybrid beam with U-shape of CFS (HUS1)	1	150 × 250 × 1300	Self-drilling screw diameter 4 mm
Hybrid beam with U-shape of CFS (HUS2)	1	150 × 250 × 1300	Square, size 1 × 1 cm

2.4 Flexural Testing

The flexural strength testing of concrete beams for all variations was conducted using a concentrated load or three-point load test. The concrete beam specimens were tested after being aged for 28 days. For the testing

Int. Journal of Integrated Engineering Vol. 17 No. 7 (2025) p. 134-143

procedure, the specimens were positioned on a loading frame with roller supports at both ends. The clear span of the beam for flexural testing was 1100 mm, and loading was applied symmetrically at the midpoint of each support to ensure pure bending. Loading was executed using a hydraulic jack equipped with load-reading indicators on the attached manometer. The loading process was gradual, with increments of 1 kN applied. Testing continued until the beam collapsed, and the load reading indicator reached its maximum value. The equipment setup and loading of the concrete beam specimens can be observed in Fig. 5.

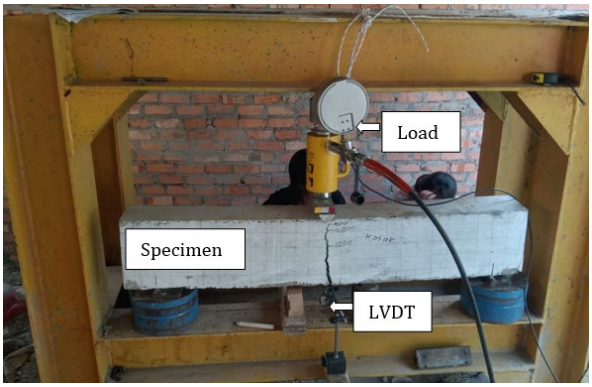

Fig. 5 *Setup of the three-point bending test*

3. Result and Discussion

3.1 Material Properties

The average concrete strength, determined from five cylindrical specimens, was 23.63 MPa, which is equivalent to a 28.5 MPa cube test. The results of tensile tests conducted on both plain reinforcement bars and 0.75 mm thick CFS are presented in Table 2.

Table 2 *Data properties of bars and CFS*

Sample	Dimension (mm)	Yield strength (MPa)	Ultimate strength (MPa)
Plain bar 5 mm	5.15	435.71	600.57
Plain bar 8 mm	7.55	374.77	531.48
CFS	12.85 × 0.75	522.11	527.60

3.2 Flexural Strength

The results of the flexural strength of the controlled beam (CB), as well as the hybrid beams with either plate-shaped or U-shaped, can be observed in Table 3. Meanwhile, the relationship between load and deflection is illustrated in Fig. 6.

Table 3 *Results of the three-point bending test*

Specimens	Load (kN)		% Change Ultimate load	Momen (kNm)	Deflection* (mm)	% Change Deflection**
	First Crack	Ultimate				
CB	12.04	23.89		6.57	11.47	
HPS1	39.91	42.49	77.86	11.68	4.86	-57.63
HPS2	22.64	33.64	40.81	9.25	2.08	-81.87
HPS3	24.72	44.75	87.33	12.31	3.75	-67.31
HUS1	32.55	42.69	78.69	11.74	6.85	-40.28
HUS2	15.32	42.71	78.78	11.75	9.7	-15.43

** Deflection at the maximum load*

*** The difference in deflection of each specimen compared to the deflection of CB*

Based on the results of the three-point bending test, it can be observed that the beams initially experienced the first crack at a load range of between 12.04 kN for the CB beam and up to 39.91 kN for the HPS1 beam. However, beams with screw shear connectors (HPS1 and HUS1) had higher first crack load values compared to beams with other types of shear connectors. The maximum load occurred in the HPS3 beam, reaching 44.75 kN, which is 87.33% higher than the CB beam. All HPS and HUS beams exhibited an increase in maximum load capacity, ranging from 40.81% to 87.33%, compared to the CB beam. As the load increased, the beams also became stiffer, as indicated by the smaller deflection that occurred at the maximum load. When compared to a previous study by Puluhulawa et al. [10], which used light steel without shear connectors, the increase in beam capacity ranged from 38.6% to 45.4%. Therefore, it can be presumed that the addition of shear connectors to light steel can enhance the bond between CFS as tensile reinforcement in concrete beams.

In terms of load-deflection profiles, both the CB beam and the HUS beams exhibit strikingly similar patterns and can be delineated into three distinct stages: pre-cracking, cracking, and post-failure. Initially, during the pre-cracking phase, all curves maintain a relatively linear trajectory until they transition into the cracking phase, where a noticeable steepening occurs, leading to the peak load. Subsequently, the post-failure phase ensues, characterised by a decline in load accompanied by an increase in deflection. Notably, these phases occur at disparate load values for the CB beam and the HUS beams, suggesting that the latter possesses a superior load-carrying capacity attributed to the incorporation of CFS as flexural reinforcement.

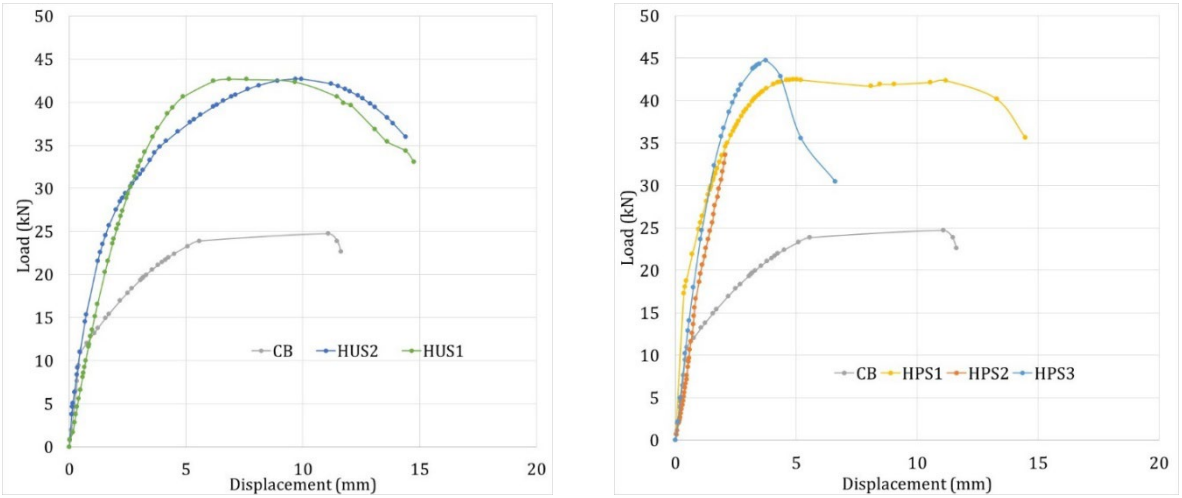

(a) **(b)**

Fig. 6 *The relationship between load and deflection (a) CB vs HUS beams; (b) CB vs HPS beams*

Fig. 6(a) highlights that regardless of the type of shear connectors employed in the HUS beams (whether screws or squares), no significant disparity in capacity is observed. This emphasises that the choice of shear connectors has a minimal influence on load capacity. In Fig. 6(b), the load-deflection profiles are shown for the CB beam and the HPS beams. Generally, the HPS beams exhibit superior ultimate stiffness compared to the control beams, indicating their enhanced ability to withstand loads. Additionally, variations in the shape of shear connectors in plate-shaped beams demonstrate a negligible impact on capacity enhancement. Consequently, it is deduced that the integration of CFS with augmented shear connectors enhances the load-bearing capacity of concrete beams.

It was observed that the beams with plate-shaped and triangle shear connectors demonstrate superior load-bearing capacity compared to other beam configurations. Conversely, the beams with plate-shaped and square shear connectors display minimal deflection at maximum load relative to other beams. It can be understood that incorporating CFS as tensile reinforcement enhances the maximum load-bearing capacity of beams. Notably, beams with identical shear connectors but different CFS profiles (plate-shaped and U-shaped) exhibit nearly identical curve shapes, albeit with the beams with plate-shaped demonstrating greater stiffness compared to the beams with U-shaped.

3.3 Comparison of Experimental to Theoretical

Table 4 presents a comparison between the experimental ultimate loads and the theoretical ultimate loads. The theoretical loads for the CB beam were computed using the Whitney Rectangular Stress Distribution Method, incorporating actual data from tested concrete and steel components. Similarly, for the hybrid beams, the same methodology as for the CB beam was employed, albeit with the incorporation of CFS in the tensile zone, assessed relative to the distance from the compression block stress. It is observed that the ratio between the experimental

Int. Journal of Integrated Engineering Vol. 17 No. 7 (2025) p. 134-143

load and the theoretical analysis load ranges from 0.67 to 0.95. The CB beam has the highest ratio, which is 0.95. This value indicates that the theoretical analysis can be used as a reference during implementation. In the case of the HUS beams, the obtained ratio values are the same, at 0.94, implying that the shape of the shear connector does not significantly influence this ratio. However, the type of CFS used can affect this ratio, as evidenced by the HUS beams having a higher ratio compared to the HPS beams.

Table 4 *Ratio of ultimate load from experimental and theoretical*

Method	Specimens					
	CB	HPS1	HPS2	HPS3	HUS1	HUS2
Theoretical ultimate load (kN) (T_{ul})	25.07		49.92		45.56	
Experimental ultimate load (kN) (E_{ul})	23.89	42.49	33.64	44.75	42.69	42.71
Ratio = E_{ul}/T_{ul}	0.95	0.85	0.67	0.90	0.94	0.94

3.4 Ductility

Various definitions of ductility and ductility indices exist for traditional reinforced concrete (RC) structures using only steel rebars. Ductility in these structures is often defined as the ratio of the deflection at the ultimate load to the deflection at the yield load. However, in the case of CFS materials, which exhibit a linear stress-strain relationship until failure and a linear energy release pattern, this differs from traditional steel reinforcement. Consequently, in this study, ductility is evaluated based on the energy theory as proposed by Hadi et al [15]. Ductility (μE) was determined using Eq. (1) by analysing the load-deflection profiles observed during the testing.

$$\mu_E = \frac{1}{2}\left(\frac{E_T}{E_{el}} + 1\right) \tag{1}$$

where $E_T = E_{inel} + E_{el}$ is the total energy, E_{inel} represents plastic energy, and E_{el} represents elastic energy. E_{inel} and E_{el} can be derived from the load-deflection profiles of the hybrid-RC beams. According to Wei et al. [16], there are two methods for determining ductility based on the load-deflection curves, as shown in Fig. 7.

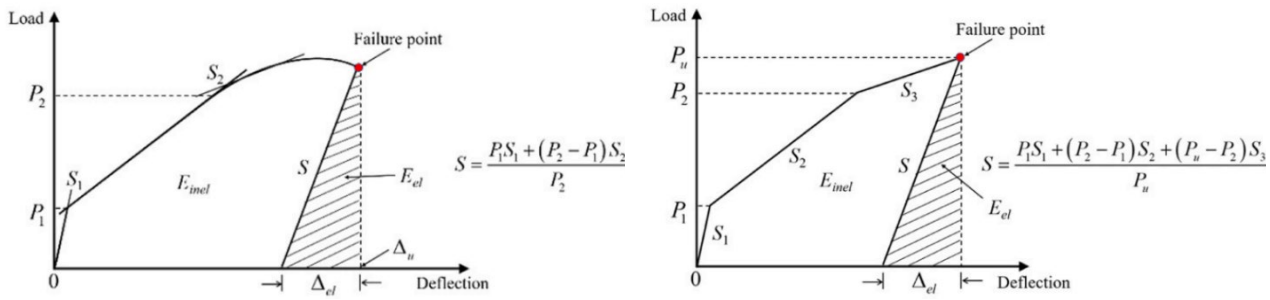

(a) (b)

Fig. 7 *Determine E_{el} based on load-deflection profile by considering - (a) Load reduction; and (b) Curve only up to the peak load*

Table 5 *Ductility of the beams*

Specimens	Slope			Load			ET	Eel	Ductility	% Change*
	S1	S2	S	P1	P2	Pu				
CB	23.16	2.54	11.99	10.94	23.88	24.73	231.55	25.51	5.04	
HPS1	52.28	9.46	30.07	17.28	35.90	42.49	161.27	30.02	3.19	-36.77
HPS2	19.72	13.26	16.84	18.64	33.64	33.64	38.08	33.60	1.07	-78.83
HPS3	23.47	11.88	18.78	23.66	39.75	44.75	116.15	53.32	1.59	-68.46
HUS1	12.76	7.12	10.91	24.16	36.02	42.69	208.69	83.55	1.75	-65.29
HUS2	17.16	1.85	9.82	21.61	41.52	42.71	326.03	92.88	2.26	-55.24

** The difference in ductility of each specimen compared to the ductility of CB*

From Table 5, it can be observed that all beams with the addition of CFS experienced a reduction in ductility values, ranging from 36.77% to 78.83%. This suggests that strengthening hybrid beams with CFS can reduce the ductility of the beams. This condition is supported by Hadi & Yuan. [15] and Pang et al. [17], who indicate that the addition of reinforcement ratio with materials having higher tensile strength can decrease the ductility of hybrid beams. The lowest ductility value is found in the HPS2 beam, which is attributed to its smaller deflection compared to the others. Beams with nearly the same Pu values (HPS1, HUS1, and HUS2) exhibit varying ductility values due to differences in deflection. This variance affects the ratio comparison between E_T and E_{el}. In conclusion, the use of shear connectors in CFS has the effect of improving the bond between CFS and concrete, thereby reducing ductility values.

3.5 Failure Mode

The crack patterns observed in the beams during flexural testing are depicted in Fig. 8. The findings show that nearly all beams experienced pure flexural failure, with cracks appearing exclusively in the middle of the span. However, beam HPS3 exhibited a flexural-shear failure, evident from diagonal cracks extending from the supports towards the load. This occurred because HPS3 sustained a load 87.33% higher than CB, exerting considerable shear force on the specimen. The stirrups' capacity proved inadequate to resist this load, leading to diagonal shear damage.

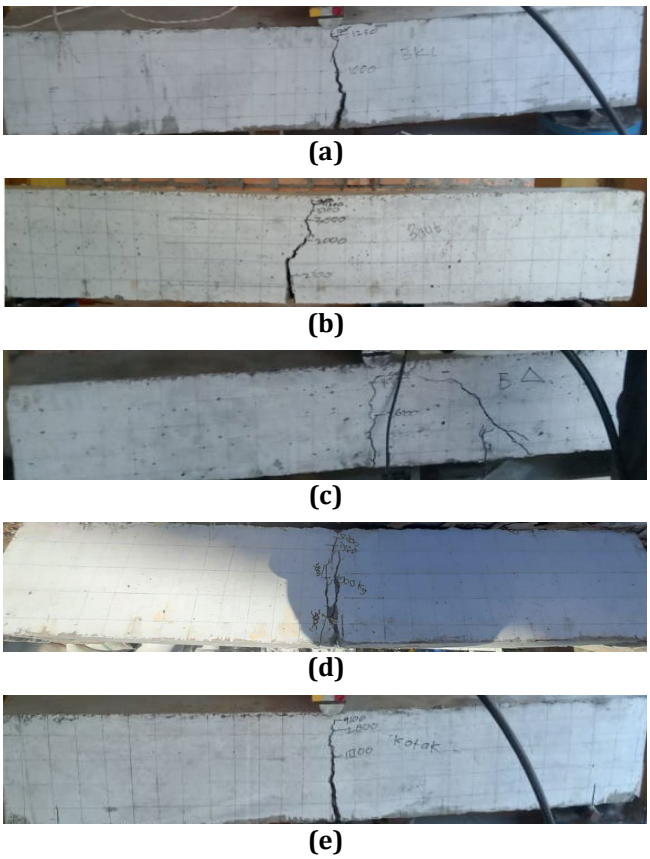

Fig. 8 *Crack pattern - (a) CB; (b) HPS1; (c) HPS3; (d) HUS1; and (e) HUS2*

4. Conclusion

The conclusions drawn from the application of shear connectors to CFS for modifying the CFS section as a strengthening material in hybrid beams are as follows:

- All beams with added shear connectors showed a notable increase in load-carrying capacity, ranging from 40.81% to 87.33%, compared to the control beams.
- The addition of shear connectors to the CFS can reduce deflection ranging from 15.4% to 81.9% compared to the control beams.
- All beams with added shear connectors experienced a reduction in ductility compared to the control beams.
- The predominant failure mode observed in all beams was flexural failure, except for the HPS3 beam, which exhibited flexural-shear failure.

Acknowledgement

This study received support from P3M Politeknik Negeri Bengkalis. The authors extend their gratitude to the staff of the Material Laboratory in the Civil Engineering Department.

Conflict of Interest

The authors declare that they have no conflict of interest regarding the publication of this paper.

Author Contribution

The authors' contributions to the paper are as follows: ***Study conception and design:*** *Indriyani Puluhulawa;* ***Data collection****: Ajeng Listianti;* ***Analysis and interpretation of results****: Indriyani Puluhulawa and Alamsyah;* ***Draft manuscript preparation****: Indriyani Puluhulawa. All authors critically reviewed the results and approved the final version of the manuscript.*

References

[1] Khala, C. C. S., Basyaruddin, Muslimin, M. S., & Putri, A. P (2021). Uji lentur balok beton bertulang baja ringan dengan skema tulangan tunggal. Teras Jurnal. https://doi.org/10.29103/tj.v11i1.418

[2] Alenezi, K., Alhajri, T., Tahir, M. M., Badr, M. R. K., & Bamaga, S. O (2013). Strengthen of cold-formed steel column with ferrocement jacket : Push out tests. International Journal of Civil, Environmental, Structural, Construction and Architectural Engineering, 7, 868–871.

[3] Taheri, E., Firouzianhaji, A., Mehrabi, P., Hosseini, B. V., & Samali, B (2020). Experimental and numerical investigation of a method for strengthening cold-formed steel profiles in bending, Applied Sciences (Switzerland). https://doi.org/10.3390/app10113855

[4] Puluhulawa, I., & Alamsyah (2020). Behavior of shear connector variations on strengthened reinforced concrete slabs using cold formed steel. IOP Conference Series: Earth and Environmental Science. https://doi.org/10.1088/1755-1315/498/1/012050

[5] Kadir, A., Satyarno, I., & Awaludin, A. (2021). Kekuatan lateral dinding cold-formed steel strap braced pada rumah instan sehat baja ringan (Risbari). Proceedings of CEEDRiMS 2021, pp. 136-143.

[6] Sifan, M., Gatheeshgar, P., Nagaratnam, B., Poologanathan, K., Navaratnam, S., Thamboo, J., & Corradi, M. (2022). Shear performance of lightweight concrete filled hollow flange cold-formed steel beams. Case Studies in Construction Materials. https://doi.org/10.1016/j.cscm.2022.e01160

[7] Khadavi, Tahir, M. M., Salih, M. N. A., Abraham Ahmad, S. A., & Shek, P. N. (2020). Behaviour of composite beam arranged as boxed-section with c-channel of cold-formed steel of lipped section. IOP Conference Series: Materials Science and Engineering. https://doi.org/10.1088/1757-899X/849/1/012073

[8] Zand, A. A. W., Alghaaeb, M. F., Liejy, M. C., Mutalib, A. A., & Al-Ameri, R. (2022). Stiffening performance of cold-formed C-section beam filled with lightweight-recycled concrete mixture. Materials. https://doi.org/10.3390/ma15092982

[9] Puluhulawa, I., Alamsyah, A., & Husna, R. (2022). The behavior of reinforced concrete beams added cold-formed-steel as shear reinforcement. Journal of Structural Monitoring and Built Environment. https://doi.org/10.30880/jsmbe.2022.02.01.002

[10] Puluhulawa, I., Alamsyah., Tifani, E., & Runandhani, V. (2023). Enhancement of reinforced concrete beam capacity by adding cold-formed steel as tensile reinforcement. Proceedings of the 11th International Applied Business and Engineering Conference. http://dx.doi.org/10.4108/eai.21-9-2023.2342916

[11] Irwan, M. J., Hanizah, A. H., & Azmi, I. (2009). Test of shear transfer enhancement in symmetric cold-formed steel-concrete composite beams. Journal of Constructional Steel Research. https://doi.org/10.1016/j.jcsr.2009.07.008

[12] SNI 03-2834-2000 (2000). Procedure for Creating A Mixed Plan Normal Concrete. Indonesian National Standard.

[13] Cui, C., Song, L., Liu, R., Liu, H., Yu, Z., & Jiang, L. (2022). Shear behavior of stud connectors in steel bridge deck and ballastless track structural systems of high-speed railways. Construction and Building Materials. https://doi.org/10.1016/j.conbuildmat.2022.127744

[14] Lin, X. M., Yam, M. C. H., Song, Y., Chung, K. F., Ho, H. C., & Han, Y. (2024). Net section tension capacity of high strength steel single shear bolted connections. Thin-Walled Structures. https://doi.org/10.1016/j.tws.2023. 111371

[15] Hadi, M. N. S., & Yuan, J. S. (2017). Experimental investigation of composite beams reinforced with GFRP I-beam and steel bars. Construction and Building Materials. https://doi.org/10.1016/j.conbuildmat.2017.03.217

[16] Wei, B., He, X., Zhou, M., Wang, H., & He, J. (2024). Experimental study on flexural behaviors of FRP and steel bars hybrid reinforced concrete beams. Case Studies in Construction Materials. https://doi.org/10.1016/j.cscm.2023.e02759

[17] Pang, L., Qu, W., Zhu, P., & Xu, J. (2016). Design propositions for hybrid FRP-steel reinforced concrete beams. Journal of Composites for Construction. https://doi.org/10.1061/(asce)cc.1943-5614.0000654